SCIENTIFIC REPORTS

natureresearch

Check for updates

OPEN

Revealing excess protons in the infrared spectrum of liquid water

Vasily G. Artemov[1✉], Ece Uykur[2], Seulki Roh[2], Artem V. Pronin[2], Henni Ouerdane[1] & Martin Dressel[2]

The most common species in liquid water, next to neutral H_2O molecules, are the H_3O^+ and OH^- ions. In a dynamic picture, their exact concentrations depend on the time scale at which these are probed. Here, using a spectral-weight analysis, we experimentally resolve the fingerprints of the elusive fluctuations-born short-living H_3O^+, DH_2O^+, HD_2O^+, and D_3O^+ ions in the IR spectra of light (H_2O), heavy (D_2O), and semi-heavy (HDO) water. We find that short-living ions, with concentrations reaching ∼ 2% of the content of water molecules, coexist with long-living pH-active ions on the picosecond timescale, thus making liquid water an effective ionic liquid in femtochemistry.

H_3O^+ and OH^- ions, characterized by picosecond-scale lifetimes in liquid water[1], are important species in biology, chemical physics, and electrochemistry, as they drive the charge transfer process and acid-base reactions in aqueous solutions, and serve as intermediates for protonic transport[2,3]. Their study dates back as early as 1806 when Grotthuss published his far-sighted theory of water conductivity[4]. Since then hydronium and hydroxide ions have been intensively investigated, yet their dynamical properties (i.e., the faster, femtosecond-scale, fluctuations) remain elusive though, thus precluding the detailed understanding of the exact ions' role in the microscopic properties of liquid water.

The presence of ionic species in pure water has been confirmed by electrochemical measurements, and their infrared (IR) and Raman spectral signatures have been found experimentally in aqueous solutions and hydrated hydronium clusters[5,6]; however the assignment of the water ions to actual (observable) spectral features of pure water are, in fact, still crucially missing[7–10]. For example, nuclear magnetic resonance, potentiometry, and conductometry are low-speed methods and hence provide only limited information on water's microscopic properties. The faster techniques, e.g., pump-probe[11], terahertz[12], and IR[13] spectroscopy are better suited to probe ultra-fast (sub-picosecond) dynamics, but miss the characteristic features of the water ions because of their low concentrations compared to that of the neutral H_2O molecules, causing the ions' spectral signatures to be hidden[14]. The dynamics of water ions has been intensively studied by theory, and particularly important results have been obtained by numerical simulations[15,16].

Femtosecond fluctuations of molecules, causing the proton transfer reactions[17], lead to the spontaneous formation of short-living (SL, denoted with *) ions, H_3O^{+*} and OH^{+*}[18], which differ from the "conventional" long-living (LL) ions, as only the latter contribute to pH and are detectable with slow measurement techniques. The formation-recombination pathway of SL ions is intermolecular and loop-shaped[19], and it yields "instantaneous" SL concentrations much higher than LL's ones[20–22], but random thermal disturbances allow transfer of SL ions to the LL pH-active H_3O^+ and OH^- ion populations[23, 24]. Importantly, because of their short lifetime (∼ 3 ps) SL ions contribute only little to dc conductivity[25,26], yet their concentration can be sufficiently large (∼ 1 M) to drive the Debye relaxation of water[22,25].

Since on time scales shorter than picoseconds, water's chemical composition can be described in terms of ionic and molecular species, both LL and SL ions should contribute to the IR (and higher energy) spectrum. However, the structure of liquid water IR spectrum is such that it cannot be used for the direct identification of the ions' contributions because of strongly overlapping bands with multiple contributions, as demonstrated in[27]. Moreover, ionic vibrations, which are absent in water vapor[28] and cannot be easily identified in the condensed phase, are entangled with intramolecular oscillations in liquid water[29]. Interpretations of liquid water's IR spectrum up

[1]Center for Energy Science and Technology, Skolkovo Institute of Science and Technology, Moscow, Russia 121205. [2]1. Physikalisches Institut, Universität Stuttgart, 70569 Stuttgart, Germany. ✉email: v.artemov@skoltech.ru

1
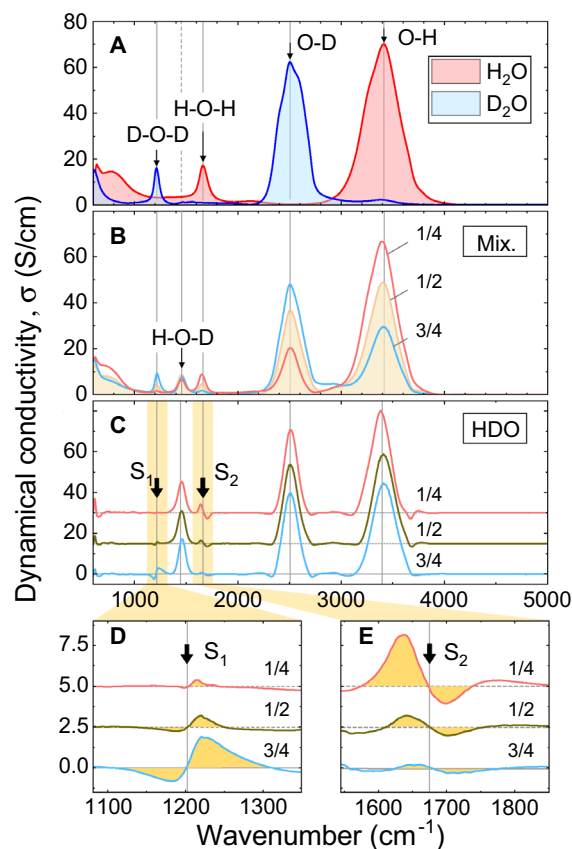
Figure 1. Experimental spectra of dynamical conductivity $\sigma(\nu)$ of (**A**) pure light and pure heavy water, (**B**) mixtures of light and heavy water with different molar isotopic fractions f as indicated, (**C**) pure HDO calculated using Eq. (1), and (**D,E**) magnified parts of the HDO spectra near the D−O−D and H−O−H bending modes showing "S-shaped" mismatches (see text). The spectra for $f = 1/2$ and $f = 1/4$ in panels (**C**–**E**) are shifted upwards for clarity. Thin arrows show two stretching modes above $2,000\ cm^{-1}$, and three bending modes below $2,000\ cm^{-1}$. Vertical lines are guides for the eye. Thick arrows indicate the areas, where the mismatches of the spectra, S_1 and S_2, occur.

to now available hence appear to necessarily rely on sophisticated analyses and models; here, following the *lex parsimoniae* principle, we attempt to derive a simple interpretation to provide a straightforward, more transparent physical picture.

In this work, we perform Fourier transform IR spectroscopy experiments of liquid light, semi-heavy, and heavy water; we analyze the data obtained with a model of the dynamical structure of liquid water, to elucidate the elusive ionic contributions to its IR spectrum. In comparison with previous studies[5,6], we study water itself, rather than aqueous solutions or other multicomponent systems, to detect the ionic species in the natural bulk water environment. The replacement of protons (one or several) in the ionic species by deuterons, shifts spectroscopic lines and makes ionic species "visible" in the integral spectrum. The spectral-weight analysis shows that up to picosecond timescale water is composed of a significant amount of short-living ionic species, influencing the nature of intermolecular interactions on this ultra-short time scale.

Results and analysis

Spectra. Figure 1A,B shows the experimental transmission infrared (TIR) spectra of dynamical conductivity $\sigma(\nu)$ for the water mixtures with different molar fractions, $f = D/(H + D)$, of heavy (D_2O) water ($0 \leq f \leq 1$). Here, D and H represent the concentrations of deuterons and protons, respectively. Details of the measurement procedure are given in the Methods section. Analyzing the absorption spectra in terms of dynamical conductivity has an important advantage: the integral under a mode in the $\sigma(\nu)$ curve is directly proportional to the number of charges involved in the absorption mechanism responsible for this mode[30,31], e.g., in corresponding vibration or rotation. This allows one to account for the concentration of species that contribute to the certain mode. One can clearly see the two groups of vibrational bands: at 1,000–2,000 and 2,000–4,000 cm^{-1}. The central frequencies and integral intensities of these bands are presented in Table 1. The right-side portion of the spectrum (frequencies above 2,000 cm^{-1}) contains the O−H and O−D stretching modes, while the left-side portion (below 2,000 cm^{-1}) hosts the H−O−H, D−O−D, and H−O−D bending modes[32]. Obviously, the H−O−D modes appear only in spectra of H_2O/D_2O mixtures (see Fig. 1B). All bands are intense, wide, and possess complex internal structures

f	DOD	HOD	HOH	OD	OH
0	n/a	n/a	1,658	n/a	3,414
			(3,360)		(29,745)
1/4	1,217	1,461	1,651	2,510	3,413
	(216)	(789)	(916)	(4,800)	(24,552)
1/2	1,217	1,457	1,653	2,509	3,410
	(385)	(961)	(509)	(8,913)	(16,822)
3/4	1,214	1,458	1,651	2,507	3,396
	(735)	(793)	(215)	(13,303)	(10,023)
1	1,213	n/a	n/a	2,506	n/a
	(1,554)			(19,351)	

Table 1. Frequencies ν in cm^{-1} (upper rows) and integral intensities I in S cm^{-2} (in brackets on lower rows) of the bending and stretching vibration peaks shown in Fig. 1 of the main text.

(consisting of several Lorentzians). The relative shift of the H_2O and D_2O lines well matches the shift of the normal modes of the corresponding harmonic oscillators (see Supplementary Information).

While the spectra of light and heavy water can easily be obtained in an experiment, the "actual" spectrum of HDO cannot be measured directly. In order to pinpoint the HDO modes, spectra of the mixtures can be analyzed as weighted sums of the spectra of light, heavy, and semi-heavy water[33,34]; hence, we may write the dynamical conductivity spectra of mixtures $\sigma_{\mathrm{mix}}(\nu, f)$ with different f as:

$$\sigma_{\mathrm{mix}}(\nu, f) = a\sigma_{\mathrm{D_2O}}(\nu) + b\sigma_{\mathrm{H_2O}}(\nu) + c\sigma_{\mathrm{HDO}}(\nu) \tag{1}$$

where $\sigma_{\mathrm{D_2O}}(\nu)$, $\sigma_{\mathrm{H_2O}}(\nu)$, $\sigma_{\mathrm{HDO}}(\nu)$ are f-independent spectra, and the coefficients $a = f^2$, $b = (1 - f)^2$, and $c = 2f(1 - f)$, are the probabilities of formation of D_2O, H_2O, and HDO, respectively. As the zero point energy difference between H and D leaves the *bending* coordinate unchanged from the normal coordinate[35], the HDO spectrum calculated from Eq. (1) should be f-independent.

Figure 1C shows spectra of HDO calculated using Eq. (1) from the spectra displayed in Fig. 1A,B. Hereinafter, we concentrate entirely on the analysis of the bending modes to avoid any influence of Fermi resonances, which are known to affect the higher frequency stretching vibrations, but are not expected to provide any significant distortions to the bending modes as these modes are those with the lowest eigenfrequencies among all vibrations. We note that the processes affecting the shapes of the bending modes and discussed in detail below, can also affect the shapes of the stretching modes. However, we do not discuss the stretching modes here, because the point of our study is not to precisely describe the entire spectrum of water, but to use this spectrum as a tool in determining the content of different ions on fast time scales. For this purpose, the bending modes are much better suited.

The HDO bending spectra generally coincide with each other; however, there are very characteristic mismatches (S-shaped features) near the D−O−D and H−O−H bands (Fig. 1C). The presence of these S-features suggests either that the measured spectra are not accurate enough, species other than H_2O, D_2O, and HDO, are present in the mixture, or substitution of H_2O by D_2O affects anharmonic resonances. We are inclined to consider the second scenario for the following reasons. First, we found that in our measurements, the intensities of the mismatches shown in Fig. 1C surely exceed the uncertainty of the transmission mode (TIR) measurements and the error of spectra processing (see Supplementary Information). Next, very similar S-shape mismatches in the HDO spectra obtained in the same frequency region have been reported earlier[33,34]. Most importantly, the frequency, and amplitude of the S-features are reproducible and consistently changing with the molar fraction f. Furthermore, the S-feature near the D−O−D bend (Fig. 1D) is mirror-symmetric in shape with respect to the S-feature near the H−O−H bending mode (Fig. 1E). This observation is in contrast to one of the previous studies[33], where both S-features are shown identical; but it is in agreement with a more precise recent study[34], where the similar pattern of the S-features were demonstrated at the analysis of absorption spectrum. Finally, the ratio between the integral intensities of the positive and negative components for the S-feature (see Figs. 1D,E) is 3:1, independently on the molar fraction f. From these points we conclude that the S-features are due to internal species of liquid water that are not taken into account by Eq. (1), as this relation includes only molecular components. Below we argue that short-lived intrinsic ions of water are good candidates for the missing water species and that the density of these ions is relatively high.

Chemical composition of liquid water. Figure 2A depicts nine principal species—neutral molecules and ions—for mixtures of light and heavy water. The species H_2O, H_3O^{+*}, OH^{-*} (group 1) and their deuterated isotopologues D_2O, D_3O^{+*}, OD^{-*} (group 2) constitute pure light and heavy water, respectively. The species HDO, HD_2O^{+*}, DH_2O^{+*} (group 3) are only present in water mixtures, where they coexist with the six species of the groups 1 and 2. Thus, in addition to the three molecular species (line i of Fig. 2A), a mixture contains also four positively charged ions (line ii) and two negatively charged ions (line iii). The relative proportion of these nine species is determined by the autoionization-recombination events, but it also depends on the molar
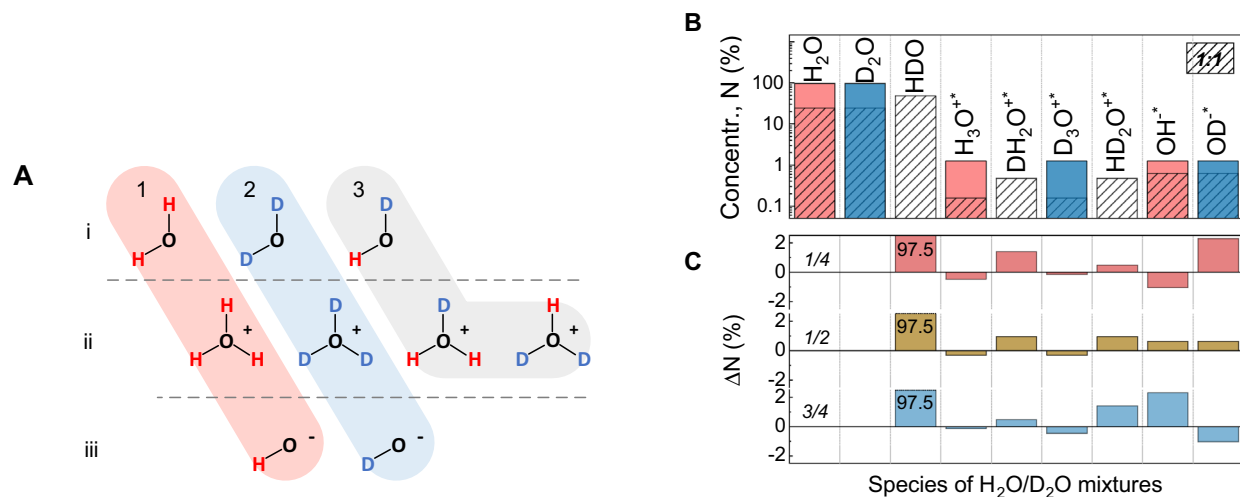
Figure 2. (**A**) Nine principal water species, present in light and heavy water (groups 1 and 2, respectively), and in their mixtures (all three groups). The rows correspond to neutral molecules (row i) and positively (row ii) and negatively (row iii) charged ions. (**B**) Percentage of the water species in pure H_2O (red), pure D_2O (blue) and their 1:1 mixture (shaded) according to Table 4; note the logarithmic scale on the *y*-axis. (**C**) Differences in ion concentrations obtained after subtraction of the normalized bars for pure light and heavy water (red and blue) from the ones for the mixtures (shaded), according to Eq.(1). Numbers near zero-lines are the molar fractions *f*. The data shown in panel (**B**) correspond to the middle raw in panel (**C**).

fraction *f*. Here and below, we do not distinguish the SL ions and LL ions: albeit their lifetimes differ, they are indistinguishable on the short timescales relevant for IR vibrations.

Inasmuch as it is difficult to detect concentration the SL ions in water directly, we rely on studies based on the terahertz absorption measurements[21], as well as on molecular dynamics simulations that take into account the auto-dissociation events in the frame of the semi-classical approach[26]. Both studies conclude that the approximate concentration of the SL ions is about 1 M (or about 2%). In a more recent investigation[22]—based on the analysis of broadband spectrum of water—the concentration of ionic species accounts to 2.5%. Hereinafter we choose this value for our preliminary analysis, and it will be later confirmed by the fit of the experimental data.

Table 4 lists the calculated percentage of nine principal species ("particles") of water mixtures for different molar fractions *f*. The concentrations of the particles are obtained by the combinatorial probability of permutation of H and D atoms around the oxygen atom O in the assumption that: (1) the probabilities for formation of the covalent H and D bonds are the same; (2) the relative percentages of ions and molecular species are identical for all mixtures; (3) the SL ions concentration is $n_i = 2.5\%$; and (4) the concentration of positively charged ions is equal to the concentration of negatively charged ions, $n^+ = n^- = n_i/2$ (charge-neutrality). The concentrations of positively charged ions are calculated from the total concentration n^+ of positive ions using the following coefficients $\alpha = (1 - f)^3$, $\beta = f^3$, $\gamma = 3f(1 - f)^2$, and $\delta = 3f^2(1 - f)$ for H_3O^{+*}, D_3O^{+*}, DH_2O^{+*}, and HD_2O^{+*}, respectively. These coefficients are the probabilities to form these ions from H and D atoms available in the mixtures. We obtained the concentrations of negatively charged ions n^-, using f and $(1 - f)$ as probability coefficients for OH^{-*} and OD^{-*}, respectively.

Figure 2B presents the concentration bars for all 9 possible species in light water ($f = 0$), heavy water ($f = 1$) and their 1:1 mixture ($f = 1/2$). The column bars correspond to the values given in Table 4. As long as the total concentrations of positive and negative ions (charges) n^+ and n^- are fixed, they are distributed among a larger number of different species (types of ions) in a mixture than in pure H_2O or D_2O. For example, the population density of OH^{-*} of pure light water in the mixture is distributed between OH^{-*} and OD^{-*}. The same for positively charged species: the asymmetric HD_2O^{+*} and DH_2O^{+*} ions, present in the mixtures only, take a part of the total charge density from the symmetric H_3O^{+*} and D_3O^{+*} ions (see the differences between the bars for pure H_2O or D_2O and for the mixtures in Fig.2B). This effect was unaccounted for in the above IR-spectrum analysis.

When we apply the normalization coefficients *a*, *b*, and *c* (the same as in Eq. (1)) to the column bars of the pure and the mixed H_2O/D_2O, only the concentrations of *molecular* species are leveled off. For the ionic species, this is not the case: their bars (in Fig. 2B) for the pure probes and for the mixtures do not coincide. This is because the relative ratio of the ionic species and the molecular species in any mixture differs from those in pure light or heavy water. In other words, this simple normalization-subtraction procedure properly works for the molecular species only, while for the ionic species the presence of additional spectral contributions is now apparent.

Figure 2C exhibits the differences obtained after subtraction of the normalized bars for pure light and heavy water from the bars corresponding to the mixtures (for $f = 1/4, 1/2,$ and $3/4$). As one can see, the H_2O and D_2O bars are subtracted completely, and all evaluated HDO-concentration columns coincide with each other ($\Delta N = 97.5\%$), but the ionic bars differ. The number of H_3O^{+*} and D_3O^{+*} ions and the number of HD_2O^{+*} and DH_2O^{+*} ions are, respectively, over- and under-estimated. Asymmetric ions are not subtracted because they do not exist in pure light and heavy water, while concentrations of symmetric ions are over-evaluated. The same
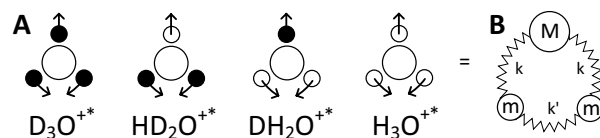
Figure 3. (**A**) Bending oscillations of positively charged ions in mixtures of light and heavy water. Black circles are D atoms, small open circles are H atom, large open circles are O atoms. (**B**) A harmonic-oscillator model representing these vibrations with the normal modes defined by Eq. (2).

	M	m	μ	k	ν_2	ν_2^{exp}
	(Da)	(Da)	(Da)	(N m^{-1})	(cm^{-1})	(cm^{-1})
H_2O	16	1	1.778	145	1,663	1,638[1]
D_2O	16	2	3.200	139	1,213	1,205[2]
H_3O^{+*}	17	1	1.789	151	1,695	1,718[3]
DH_2O^{+*}	18	1	1.800	142	1,637	No data
HD_2O^{+*}	17	2	3.238	142	1,222	No data
D_3O^{+*}	18	2	3.273	138	1195	1,194[1]

Table 2. Parameters of oscillations shown in Fig. 3 and bending normal-mode frequencies, $\nu_2 = \omega_2/2\pi$, calculated with Eq. (2), comparison with the experimental results, ν_2^{exp}.

applies for negatively charged OH^{-*} and OD^{-*} ions. Their relative concentrations in the mixture differ from those for neutral molecules, which leads to the corresponding residual bars after subtraction.

As the probability of the formation of asymmetric ions is three-times-higher than for symmetric ones, the relative ratio of the concentrations of up-going and down-going residual bars of positively charged ions in Fig. 2C is 3:1 everywhere (compare the bars for H_3O^{+*} and DH_2O^{+*}, as well as, D_3O^{+*} and HD_2O^{+*} for each probe). The ratio is the same as observed for the positive and negative parts of the experimentally observed S-features in Fig. 2. This, as well as the fact that the intensities of S-features are proportional to the concentration of ionic species, make it possible to identify ions in the spectrum and calculate their concentrations.

Assignment of the S-features. Because the OH^{-*}- and OD^{-*}-ion vibrations are very close to the O−H and O−D stretching modes, they are hidden within the bands at 2450 and 3400 cm^{-1} (see Fig. 1C). However, the positively charged ions, D_3O^{+*}, HD_2O^{+*}, DH_2O^{+*}, and H_3O^{+*} possess vibrational modes, whose frequencies are different, and also from the HDO, H_2O, and D_2O frequencies. Thus, the concentrations of the positively charged ions in the mixtures can be identified by comparing their IR spectra.

Figure 3 sketches the bending vibrations of positively charged ions, whose frequencies are expected to be close to (but still different from) the bending frequencies of H_2O and D_2O at 1650 and 1240 cm^{-1}, respectively (see Fig. 1). If we now utilize a simple harmonic-oscillator model with three masses and three springs depicted in Fig. 3, two modes with the following nonzero eigenfrequencies are expected:

$$\omega_1 = \sqrt{(2k' + k)/m} \;\; \text{and} \;\; \omega_2 = \sqrt{2k/\mu} \tag{2}$$

where k and k' are the spring constants, $\mu = 2mM/(2m + M)$ is the effective mass (which is given in Table 2 for different species of water), m is the mass of deuteron or proton, and M is the mass of one oxygen atom (plus the mass of one deuteron or proton in the case of DH_2O^{+*} and HD_2O^{+*} ions). The mode with the eigenfrequency ω_2 corresponds to bending vibrations shown in Fig. 3. The second mode is a stretching vibration and is not relevant for this study. The spring constant k' (which correspond to the vibrations between the light atoms) is close to zero, while k (the vibrations between a light atom and heavy oxygen) is equal to 142 ± 4N/m^{-1} for both H_2O and D_2O, as can be defined from the experimental frequencies of H_2O and D_2O molecules and Eq. (2)[36].

The constant k is not expected to change much across the isotopologues and from Eq. (2) one should expect that: (1) the heavier ions have lower oscillation frequencies and (2) D_3O^{+*} and HD_2O^{+*} have their vibrational frequencies close to the D_2O bending mode, while the frequencies of DH_2O^{+*} and H_3O^{+*} are close to the bending mode of H_2O. Thus, the spectral fingerprints of the ions illustrated in Fig. 3 are expected to appear in the following order with increasing frequency: H_3O^{+*}, DH_2O^{+*}, HD_2O^{+*}, and D_3O^{+*}, first two being around 1660 cm^{-1}, while the last two showing up near 1,210 cm^{-1}.

We now provide the parameterization of the observed S-features. Figure 4 explains graphically how the fits of these features were obtained. The Lorentz-oscillator parameters for the ions were acquired by performing a simultaneous fitting of the measured spectra and the corresponding S-features from Fig. 1 using the following equations:
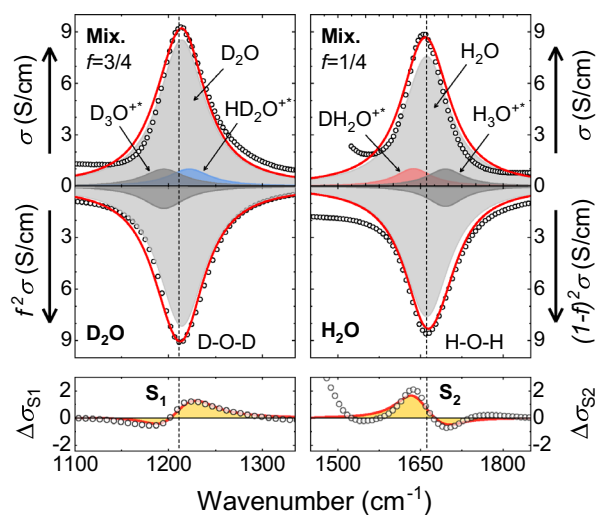
Figure 4. Examples of the S-feature fits near the bending modes. The total fits are shown as red lines, while different Lorentzian terms are represented as shaded areas. The experimental data are open symbols. Left (right) panels display the spectra near the resonances at around 1,210 (1,660) cm^{-1}. The fits are shown for the largest observed S-features (cf. Fig. 1D,E). The top row of panels shows the conductivity spectra for the $f = 3/4$ (left) and $f = 1/4$ (right) mixtures, respectively. In the middle row, the conductivities for pure D$_2$O (left) and H$_2$O (right) are shown upside down to demonstrate the subtraction procedure utilized for the S-feature fits, as described by Eqs. (3) and (4). The resultant S-feature fits are shown in the bottom panels.

	I	w	ν_2	n_i	n_i	n_i
	–	(cm^{-1})	(cm^{-1})	$f = 1/4$	$f = 1/2$	$f = 3/4$
H$_2$O	15.0	50	1,663	55	24	6
D$_2$O	13.5	27	1,213	6	24	55
H$_3$O^{+*}	3.1	40	1,695	0.53	0.16	0.02
DH$_2$O^{+*}	3.1	40	1,637	0.53	0.47	0.18
HD$_2$O^{+*}	2.3	27	1,222	0.18	0.47	0.53
D$_3$O^{+*}	2.3	27	1,195	0.02	0.16	0.53

Table 3. Parameters of the Lorentz fit according to Eqs. (3) and (4) to the experimental spectra shown in Fig. 4 and the ion concentrations n_i for different molar fractions f, as calculated using Eq. (5): I is the intensity, w is the half-width and ν_2 is the central frequency.

f	0	1/4	1/2	3/4	1
HDO	0	36.56	48.75	36.56	0
H$_2$O	97.5	54.84	24.38	6.094	0
D$_2$O	0	6.094	24.38	54.84	97.5
H$_3$O^{+*}	1.25	0.527	0.156	0.020	0
D$_3$O^{+*}	0	0.020	0.156	0.527	1.25
DH$_2$O^{+*}	0	0.527	0.469	0.176	0
HD$_2$O^{+*}	0	0.176	0.469	0.527	0
OH^{-*}	1.25	0.313	0.625	0.938	0
OD^{-*}	0	0.938	0.625	0.313	1.25

Table 4. Percentage of species (neutral molecules and SL ions) in liquid H$_2$O, D$_2$O and their mixtures.

$$\Delta\sigma_{S_1} = [f^2(\sigma_{D_2O} + \beta\sigma_{D_3O^{+*}}) + 2f(1-f)\delta\sigma_{HD_2O^{+*}}] - f^2[\sigma_{D_2O} + \sigma_{D_3O^{+*}}] \tag{3}$$

$$\Delta\sigma_{S_2} = [(1-f)^2(\sigma_{H_2O} + \alpha\sigma_{H_3O^{+*}}) + 2f(1-f)\gamma\sigma_{DH_2O^{+*}}] - (1-f)^2[\sigma_{H_2O} + \sigma_{H_3O^{+*}}] \tag{4}$$

where α, β, γ, δ are the same as defined above, and all σ_i's are functions of ν: $\sigma_i(\nu) = I_i w_i^2 / [w_i^2 + (\nu_{oi} - \nu)^2]$ is the Lorentz-oscillator contribution to the dynamical conductivity, with I_i being its intensity, w_i its half-width, ν_{oi} the oscillator central frequency, and f is the D_2O molar fraction in the water mixture, as already defined. These formulas follow from Eq. (1), if the water mixtures contain ions with the concentrations defined above (see the section "Chemical composition of liquid water") and if we apply the spectra subtraction procedure, discussed above for the experimentally obtained S-features, to our fits. The fit parameters are given in Table 3. One can see a very good agreement between the model and the experimental data. Thus, the mismatches in the subtracted HDO spectra are assigned to the SL ionic species that are parts of the IR spectra of light and heavy water, as well as their mixtures.

S-features in the subtracted spectra of HDO were already reported in[34], where spectral data were analyzed in terms of absorption $\alpha = 4\pi\sigma(\nu)/n(\nu)c$, where c is a speed of light, $n(\nu)$ is the frequency dependent refractive index; unfortunately it cannot reflect the true concentration of ionic species. Nevertheless, the residues in the HDO spectra are quite similar to ours, indirectly confirming our results. The authors interpret the residues in terms of hydrogen bonding, considering the perturbation of the intramolecular vibrations caused by surroundings, as they assumed that molecular species (H_2O, D_2O, and HDO) oscillation frequencies change by the neighboring atoms that provide hydrogen or deuterium bonds[34]. In spite of their very careful spectral analysis, this physical interpretation lacks clarity mainly because the expected concentrations of perturbed molecules are too high compared to those we observe (Fig. 4). For example, in the 1:1 mixture of light and heavy water, one expects that half of the bonds with neighboring molecules are formed by deuterons, while the residuals are too small to be explained in this way. We believe our approach to the interpretation of the IR spectra of D_2O/H_2O mixtures by introduction of the ionic species is more suitable.

Ion concentrations. Having understood the origin of the discrepancy of the "pure" HDO spectra obtained at different molar fractions f, we can calculate the concentration of ionic species in water from their S-features. The spectral weight S of a Lorentz oscillator is related to the density of charges involved in the absorption process[30,31]:

$$S_i = \int_0^\infty \sigma(\omega')d\omega' = \frac{\pi}{2}\frac{n_i q_i^2}{\mu_i} \tag{5}$$

where μ_i, q_i and n_i are the effective mass, charge, and concentration of the conducting species of the i-th kind. Taking into account the effective masses and the parameters of Lorentzians obtained above, one can calculate the concentrations of the corresponding water species. The results are summarized in Table 3. The concentrations obtained are in good agreement with the expected percentage for the different species in liquid water presented in Table 4. Thus, we have shown that the subtraction residuals shown in Fig. 1B,C correspond to the unaccounted ionic species of H_3O^{+*}, DH_2O^{+*}, HD_2O^{+*}, and D_3O^{+*}.

Discussion and concluding remarks

We have studied the infrared spectra of the H_2O, D_2O, and their mixtures in the direct transmission mode to uncover the hidden IR vibrations of water's ionic species. Our study reveals that the intramolecular vibrational dynamics observed in the IR spectrum of water is not reduced to the oscillatory motion of molecular species only. The presence of the residues on the spectrum of "pure" HDO, obtained from the mixtures with different molar fractions of light and heavy water, clearly shows that absorption of IR waves by water is partially defined by the dynamics of ionic species, whose concentration (at least at short times < 0.1 ps—the low frequency limit of TIR) is about 2% of the total number of molecules in liquid water. In order to bring this result in accord with pH concept, we suggest that fluctuation-driven short-living ions coexist with conventional long-living pH-active ions at short times of observation corresponding to the IR frequency range. The detected ionic species are important for water related processes, e.g. solvation, dissolution, osmosis, cavitation, radiolysis, which take place on short length (nanometer) and time (sub-picosecond) scales[37–39]. We believe that an account for the ionic species on the ultrashort time scale can help to improve, and significantly simplify models of physical-chemical and electrochemical systems where liquid water plays a significant role[40,41]. The space-time intervals discussed in our work are suitable for ab-initio approaches; and molecular dynamics simulations are highly welcome.

Methods

Samples of H_2O and D_2O with purity of 99.9% obtained from Sigma-Aldrich were used in this work. Probes with different molar fractions of deuterium, f, were prepared by mixing pure light and heavy water before measurements. The spectra were recorded in transmission mode[42] using a Bruker Vertex 80v spectrometer in the frequency range 600–8,000 cm^{-1}. For these measurements, a drop of water was sandwiched between two 3-mm-thick ZnSe windows. ZnSe is perfectly suited for such a type of measurements: it is hydrophobic and highly transparent with no absorption lines in the range of interest. There are no spacers between the windows. Instead, we controlled the stabilization of the water layer, measuring the IR spectra every 30 seconds until they were stabilized. The thickness for the light, heavy, and semi-heavy water samples was about 1 μm, slightly varying from sample to sample. The reference spectrum of the windows was recorded separately in advance. In order to

eliminate the multiple reflections inside the water layer, the spectra were processed using a five-media model[43] and an algorithm of least-squares minimization[44].

For our study, we intentionally chose the transmission mode (TIR) instead of the attenuated total reflection (ATR) technique[45]. Although the ATR method provides the spectra without any fringes caused by multiple reflections within the water layer, the true absorption spectrum with the absolute values of transmitted intensity is only available in the TIR. As there is a discrepancy between the liquid water spectra obtained by these two methods (Fig. 6 of the Supplementary Information), for the spectral weight analysis and the calculation of the ion concentrations a directly obtained TIR spectrum was used.

References

1. Amir, W. *et al.* Time-resolved observation of the Eigen cation in liquid water. *J. Chem. Phys.* **126**, 034511 (2007).
2. Bell, R. P. *Proton in Chemistry* (Cornell University Press, Ithaca, 1959).
3. Bodi, A., Csontos, J., Kállay, M., Borkar, S. & Sztáray, B. On the protonation of water. *Chem. Sci.* **5**, 3057 (2014).
4. de Grotthuss, C. Theory of decomposition of liquids by electrical currents. *Ann. Chim.* **58**, 54–74 (1806) (**(in French)**).
5. Falk, M. & Giguére, P. A. Infrared spectrum of the H_3O^+ ion in aqueous solutions. *Can. J. Chem.* **35**, 1195 (1957).
6. Okumura, M., Yeh, L. I., Myers, J. D. & Lee, Y. T. Infrared spectra of the solvated hydronium ion: vibrational predissociation spectroscopy of mass-selected $H_3O^+(H_2O)_n(H_2)_m$. *J. Phys. Chem.* **94**, 3416 (1990).
7. Kim, J., Schmitt, U. W., Gruetzmacher, J. A., Voth, G. A. & Scherer, N. E. The vibrational spectrum of the hydrated proton: comparison of experiment, simulation, and normal mode analysis. *J. Chem. Phys.* **116**, 737 (2002).
8. Heuft, J. M. & Meijer, E. J. A density functional theory based study of the microscopic structure and dynamics of aqueous HCl solutions. *Phys. Chem. Chem. Phys.* **8**, 3116 (2006).
9. Woutersen, S. & Bakker, H. J. Ultrafast vibrational and structural dynamics of the proton in liquid water. *Phys. Rev. Lett.* **96**, 138305 (2006).
10. Biswas, R., Carpenter, W., Voth, G. A. & Tokmakoff, A. Molecular modeling and assignment of IR spectra of the hydrated excess proton in isotopically dilute water. *J. Chem. Phys.* **145**, 154504 (2016).
11. Woutersen, S., Emmerichs, U. & Bakker, H. J. Femtosecond mid-IR pump-probe spectroscopy of liquid water: evidence for a two-component structure. *Science* **278**, 658 (1997).
12. Rønne, C., Åstrand, P.-O. & Keiding, S. R. THz spectroscopy of liquid H_2O and D_2O. *Phys. Rev. Lett.* **82**, 2888 (1999).
13. Kindt, J. T. & Schmuttenmaer, C. A. Far-infrared dielectric properties of polar liquids probed by femtosecond terahertz pulse spectroscopy. *J. Phys. Chem.* **100**, 10373 (1996).
14. Zundel, G. *The Hydrogen Bond: Recent Developments in Theory and Experiments* Vol. 2 (NorthHolland, Amsterdam, 1976).
15. Chen, M. *et al.* Hydroxide diffuses slower than hydronium in water because its solvated structure inhibits correlated proton transfer. *Nat. Chem.* **10**, 413 (2018).
16. Chandler, D. From 50 years ago, the birth of modern liquid-state science. *Annu. Rev. Phys. Chem.* **5**, 19 (2017).
17. Nagata, Y., Pool, R. E., Backus, E. H. G. & Bonn, M. Nuclear quantum effects affect bond orientation of water at the water–vapor interface. *Phys. Rev. Lett.* **109**, 226101 (2012).
18. Geissler, P. L., Dellago, C., Chandler, D., Hutter, J. & Parrinello, M. Autoionization in liquid water. *Science* **291**, 2121 (2001).
19. Codorniu-Hernández, E. & Kusalik, P. G. Probing the mechanisms of proton transfer in liquid water. *PNAS* **110**, 13697 (2013).
20. Bai, C. & Herzfeld, J. Special pairs are decisive in the autoionization and recombination of water. *J. Phys. Chem. B* **121**, 4213 (2017).
21. Volkov, A. A., Artemov, V. G. & Pronin, A. V. A radically new suggestion about the electrodynamics of water: can the pH index and the Debye relaxation be of a common origin?. *EPL* **106**, 46004 (2014).
22. Artemov, V. G. A unified mechanism for ice and water electrical conductivity from direct current to terahertz. *Phys. Chem. Chem. Phys.* **21**, 8067 (2019).
23. Hassanali, A., Giberti, F., Cuny, J., Kühne, T. D. & Parrinello, M. Proton transfer through the water gossamer. *PNAS* **110**, 13723 (2013).
24. Ceriotti, M., Cuny, J., Parrinello, M. & Manolopoulos, D. E. Nuclear quantum effects and hydrogen bond fluctuations in water. *PNAS* **110**, 15591 (2013).
25. Artemov, V. G., Volkov, A. A. & Pronin, A. V. Electrical properties of water: a new insight. *Biophysics* **59**, 520 (2014).
26. Bai, C., Kale, S. & Herzfeld, J. Chemistry with semi-classical electrons: reaction trajectories auto-generated by sub-atomistic force fields. *Chem. Sci.* **8**, 4203 (2017).
27. Riemenschneider, J. *Spectroscopic Investigations on Pure Water and Aqueous Salt Solutions in the Mid Infrared Region*. Ph.D. thesis, University of Rostock (2011).
28. Hall, R. T. & Dowling, J. M. Erratum: Pure rotational spectrum of water vapor. *J. Chem. Phys.* **54**, 4968 (1971).
29. Max, J. J. & Chapados, C. Determination of spectroscopic band shapes by second derivatives, part II: infrared spectra of liquid light and heavy water. *Appl. Spectrosc.* **69**, 1281 (2015).
30. Landau, L. D. & Lifshitz, E. M. *Electrodynamics of Continuous Media* 1st edn, 261 (Pergamon Press, New York, 1960).
31. Dressel, M. & Grüner, G. *Electrodynamics of Solids* (Cambridge University Press, Cambridge, 2002).
32. Walrafen, G. E. Raman and infrared spectral investigations of water structure. In *Water a Comprehensive Treatise* Vol. 1 (ed. Franks, F.) 151–214 (Plenum Press, New York, 1972).
33. Maréchal, Y. Infrared spectra of water. I. Effect of temperature and of H/D isotopic dilution. *J. Chem. Phys.* **95**, 5565 (1991).
34. Max, J. J. & Chapados, C. Isotope effects in liquid water by infrared spectroscopy. *J. Chem. Phys.* **116**, 4626 (2002).
35. Yagi, K., Keçeli, M. & Hirata, S. Optimized coordinates for anharmonic vibrational structure theories. *J. Chem. Phys.* **137**, 204118 (2012).
36. Wilson, E. B., Decius, J. C. & Cross, P. C. *Molecular Vibrations* 175 (McGraw-Hill, New York, 1955).
37. Ouerdane, H., Gervais, B., Zhou, H., Beuve, M. & Renault, J.-Ph. Radiolysis of water confined in porous silica: a simulation study of the physicochemical yields. *J. Phys. Chem. C* **114**, 12667 (2010).
38. Stoyanov, E. S., Stoyanova, I. V. & Reed, C. A. The unique nature of H^+ in water. *Chem. Sci.* **2**, 462 (2011).
39. Artemov, V. G. *et al.* Anomalously high proton conduction of interfacial water. *J. Phys. Chem. Lett.* **11**, 3623 (2020).
40. Wang, P., Anderko, A. & Young, R. D. Modeling electrical conductivity in concentrated and mixed-solvent electrolyte solutions. *Ind. Eng. Chem. Res.* **43**, 8083 (2004).
41. Andreev, M., de Pablo, J. J., Chremos, A. & Douglas, J. F. Influence of ion solvation on the properties of electrolyte solutions. *J. Phys. Chem. B* **122**, 4029 (2018).
42. Cowan, M. *et al.* Ultrafast memory loss and energy redistribution in the hydrogen bond network of liquid H_2O. *Nature* **434**, 199 (2005).
43. Max, J. J. & Chapados, C. Infrared transmission equations in a five media system: gas and liquid. *J. Math. Chem.* **47**, 590 (2010).

44. Kuzmenko, A. B. Kramers–Kronig constrained variational analysis of optical spectra. *Rev. Sci. instrum.* **76**, 083108 (2005).
45. Fujiyama, T., Herrin, J. & Crawford, B. L. Jr. Vibrational intensities XXV: some systematic errors in infrared absorption spectrophotometry of liquid samples. *Appl. Spectrosc.* **24**, 9 (1970).

Acknowledgements

Author contributions

V.G.A. and A.V.P. conceived the idea of the study. E.U. and V.G.A conducted the experiments, S.R., H.O., M.D., and V.G.A. analyzed the data. M.D., and H.O. supervised the project. V.G.A. wrote the manuscript. H.O, A.V.P. and M.D. reviewed and edited the manuscript. All authors discussed the results and contributed to the manuscript. All data is available upon request.

Competing interests

The authors declare no competing interests.

Additional information

Supplementary information is available for this paper at https://doi.org/10.1038/s41598-020-68116-w.

Correspondence and requests for materials should be addressed to V.G.A.

Reprints and permissions information is available at www.nature.com/reprints.

Publisher's note Springer Nature remains neutral with regard to jurisdictional claims in published maps and institutional affiliations.